Applied Radiation and Isotopes 178 (2021) 109935

Contents lists available at ScienceDirect

Applied Radiation and Isotopes

journal homepage: www.elsevier.com/locate/apradiso

A heavy-ion production channel of ^{149}Tb via ^{63}Cu bombardment of ^{89}Y

John T. Wilkinson [a,*], Kendall E. Barrett [b], Samuel J. Ferran [c], Sean R. McGuinness [a], Lauren A. McIntosh [d], Mallory McCarthy [d], Sherry J. Yennello [d], Jonathan W. Engle [b], Suzanne E. Lapi [c], Graham F. Peaslee [a]

[a] Department of Physics, University of Notre Dame, Notre Dame, IN, 46556, USA
[b] Department of Medical Physics, University of Wisconsin-Madison, Madison, WI, 53715, USA
[c] Department of Radiology, University of Alabama at Birmingham, Birmingham, AL, 35294, USA
[d] Cyclotron Institute, Texas A&M University, College Station, TX, 77840, USA

ARTICLE INFO

Keywords:
^{149}Tb
Heavy-ions
Isotope production
Theranostics

ABSTRACT

The radionuclide ^{149}Tb ($t_{1/2}$ = 4.1 h) is a potential theranostic isotope which can simultaneously be used for targeted-alpha-particle therapy and positron-emission tomography. Feasibility experiments were performed to test a near-symmetric heavy-ion reaction of ^{63}Cu bombardment on monoisotopic ^{89}Y. The indirect reaction was studied to avoid isomer production. Offline gamma spectroscopy was used to quantify thick-target physical yields and experimental results show modest agreement to the fusion-evaporation code PACE4. A near-symmetric fission yield was also observed.

1. Motivation

In recent decades, modern nuclear medicine has expanded physicians' arsenal in the fight against cancer with the development of targeted radiation therapy (TRT). TRT uses agents to transport radioactive material specifically to cancer cells. The targeting agents can be antibodies, proteins, small molecules, or simple salts containing radioactive atoms taken up by target tissue *in vivo*. Theranostic radionuclides (with dual diagnostic and therapeutic capabilities) enable noninvasive assessment of targeting efficacy and dosimetry in individual patients (Naskar and Lahiri, 2021). However, dependable production routes and infrastructure (including capable ion sources and accelerator systems) are needed to make these specialized radionuclides available for research and clinical applications.

Various decay modes have shown promise for TRT including alpha, beta, and electron capture/internal conversion. The range and linear energy transfer of emitted particles determine the effectiveness of a delivered radionuclide, with alpha particles delivering the largest dose to the smallest volume of tissue due to the high stopping power (Poty et al., 2018a). The high stopping power and short projected range spares neighboring healthy tissue in this targeted therapy (Aghevlian et al., 2017; McDevitt et al., 1998). Many suitable theranostic targeted-alpha-particle therapy (TAT) radionuclides are neutron-rich isotopes that can be difficult to obtain due to their slow production rate from generators, the difficulty of extraction from fission products, or the lack of accelerator-based production routes (Poty et al., 2018b). One potential TAT radionuclide is ^{149}Tb (Allen and Blagojevic, 1996). ^{149}Tb is not produced from fissile material and is the lightest medically useful alpha emitter with potential application as a TAT radiolabel (Poty et al., 2018b). In addition to its positron emission suitable for diagnostics with positron emission tomography (PET), the ground state of ^{149}Tb also undergoes an alpha decay which satisfies the therapeutic aspect of theranostics (Beyer et al., 2004; Müller et al., 2017). However, ^{149g}Tb production is challenging, and this inaccessibility has limited preclinical studies and clinical trials.

The production difficulty of this radionuclide with a 4.12-h half-life has restricted investigations to facilities nearest the production site to date, primarily the Isotope mass Separator On-Line (ISOLDE) facility at CERN (Beyer et al., 2004; Müller et al., 2017). The isotope production facility, CERN-MEDICIS, has achieved production of ^{149}Tb in 2018, but the distribution network will be limited because of its half-life (Duchemin et al., 2020). Difficulties in producing high purity and high yields are the greatest challenges. Terbium has four medically viable isotopes, ^{149g}Tb, ^{152}Tb, ^{155}Tb, and ^{161}Tb (Duchemin et al., 2016; Müller et al., 2014). Among these, ^{149g}Tb is the only radioisotope with both diagnostic (Total $I_{\beta+}$ = 7.1%) and therapeutic (I_{α} = 16.7%, $E_{max,\alpha}$ = 3.970 MeV) emissions (Browne and Tuli, 2009). Most production of ^{149g}Tb has been accomplished at the ISOLDE facility with GeV proton spallation

* Corresponding author. 225 Nieuwland Science Hall, University of Notre Dame, Notre Dame, IN, 46556.
E-mail address: jwilkin5@nd.edu (J.T. Wilkinson).

https://doi.org/10.1016/j.apradiso.2021.109935
Received 16 February 2021; Received in revised form 14 August 2021; Accepted 2 September 2021
Available online 14 September 2021

reactions (Beyer et al., 2002). Despite the high ^{149}Tb activity, the spallation reaction coproduces radioisotopic contaminants of terbium that require electromagnetic mass separation, like ISOLDE, to achieve purity suitable for medical applications.

The goals of this work were to investigate a heavy-ion reaction pathway to produce ^{149g}Tb and to determine the achievable yields and radioisotopic purity. Among the production challenges of ^{149}Tb is the existence of a low-lying nuclear isomer close to the ground state. The ground state nucleus has a spin and parity of $J^{\pi} = ½^{+}$ and this 4-min isomer has $J^{\pi} = \frac{11}{2}^{-}$ at just 36 keV above the ground state. The large angular momentum difference between these two states insulates the ground state from an internal transition. As a result, direct reactions at higher bombarding energies populate the isomeric state at the expense of the ground state (Macfarlane, 1962; Morton et al., 1962). Therefore, in this study an indirect production pathway was chosen for its increased production of the medically useful ground state. Specifically, the decay of the parent isotope, ^{149}Dy, populates the ground state of ^{149}Tb in 52% of decays, and this has been shown to yield higher specific activities than direct production alone (Beyer et al., 2002; Firestone et al., 1996). We irradiated yttrium targets with a ^{63}Cu beam and measured formation of ^{148}Tb, ^{149}Tb, and ^{150}Tb via offline gamma-ray spectroscopy. By limiting the nucleons available within the reaction, this heavy-ion route was predicted by PACE4 to offer higher nuclide selectivity and avoid many other byproducts from spallation reactions, especially for bombarding energies just above the Coulomb barrier. Fig. 1 shows the fusion-evaporation production channel investigated in this work.

2. Materials & methods

2.1. Reaction modeling

The fusion-evaporation code PACE4, a statistical model of nuclear reactions within the LISE++ framework, simulated all reaction cross-sections (Gavron, 1980). LISE++ was designed to simulate intensities and transmission of fragments in a fragment separator, like the National Superconducting Laboratory (NSCL), but encompasses a Monte-Carlo code for fusion-evaporation of nuclear residues, which is PACE4. PACE4 is an analytical approximation of PACE described in Gavron, 1980, that couples angular momenta to a modified version of JULIAN (Tarasov and Bazin, 2003). For each beam-target pair, the bombarding energy was varied over a range of 70 MeV, increasing from the Coulomb barrier to determine optimal bombarding energies. Each cascade calculation was run for 100,000 iterations which kept statistical error about 1%. Convergence was clear beyond 10,000 iterations, but additional iterations were run to minimize simulation error. The modeling was chosen to simulate energies from the Coulomb barrier (229 MeV) up to an optimized bombardment energy for an energetically thick target.

Both ^{148}Tb and ^{150}Tb, with half-lives of 1-h and 3.5-h, respectively, are not considered attractive medical isotopes but may be suitable for chemistry development. The neighboring daughters, ^{148}Gd and ^{150}Gd, are undesirable coproducts due to long half-lives of 70.9 and 1.8×10^{6} years, respectively. In addition to ^{149}Tb production, measurements of all produced terbium isotopes was a secondary focus due to the inability to chemically separate these contaminants. The model predictions were used to select an optimal beam-target pair and bombarding energy that would minimize contaminant terbium isotope production, since any purification and separation from the target cannot isolate these. This proof-of-concept work only considers thick-target yields, accepting all reactions from the bombarding energy down to the Coulomb barrier, with the beam stopping in the target. Limiting considerations to near-barrier reactions, the A = 150, or heavier mass chain, could then be minimized by limiting the total number of involved nucleons. The most suitable reaction pathway was ^{89}Y (^{63}Cu, *xn yp*)^{149}X, where ^{149}Tb is primarily produced indirectly such as in ^{89}Y (^{63}Cu,*p2n*)^{149}Ho and ^{89}Y (^{63}Cu,*3n*)^{149}Er. The copper beam incident on yttrium produces the compound nucleus ^{152}Er and subsequent exit-channel products as shown in Fig. 1. In this scheme, any isobaric parent could be the nucleus of interest, as all have decay modes of electron capture or β^{+} emission and will decay to ^{149}Tb. The indirect reaction pathway achieves the highest production of the desired ground-state nucleus ^{149}Tb by allowing one or more A = 149 radionuclides to serve as the immediate reaction product. Additionally, yttrium (as a target material) is naturally monoisotopic and has a high melting point (1522 °C), and 100% purity in the beam is easily achieved by maximizing ^{63}Cu transmission through the ion source and cyclotron. The statistical evaporation of just a few nucleons from ^{152}Er was the greatest factor in minimizing heavier contaminants.

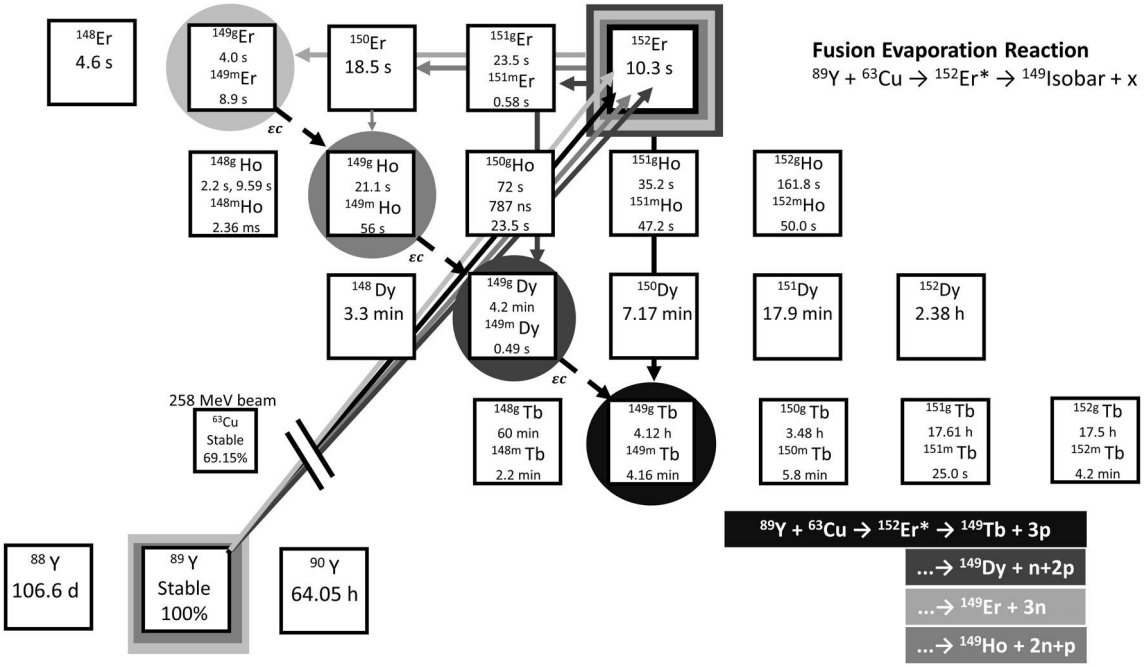

Fig. 1. Indirect fusion-evaporation model.

2.2. Experimental design

Irradiations were performed at Texas A&M's Cyclotron Institute using the K150 cyclotron (Tabacaru et al., 2019; Radiation Effects Facility, 2020). The ^{89}Y (^{63}Cu, *xn yp*)^{149}X reaction has a Coulomb barrier of 229 MeV, and the maximum desired beam energy for this study was 258.0 ± 0.5 MeV, or 4.1 MeV/A ± 0.2%. The cyclotron operated on a third harmonic frequency to achieve the low bombarding energy for copper. About 10 electrical-nA of ^{63}Cu were delivered in the 15+ charge state. The consistency of the beam delivery was high, as during periodic beam current checks 97% of the recorded values were within 15% of the beam current weighted average for each irradiation.

A target mount was custom designed and fabricated at the University of Notre Dame using aluminum holders to affix a 1 mm thick, 25 × 25 mm^2 yttrium target onto an ISO-KF100 blank flange. For this experiment, the cyclotron energy remained fixed to minimize retuning between irradiations, and a degrader foil method was used to moderate bombarding energies from the fixed third harmonic beam energy. Aluminum foil degraders were chosen for their availability, low cost, and relatively small attenuation. For each bombardment, only one yttrium target was irradiated within the stack, and the beam was calculated to stop within the first 30 μm of the target (Ziegler et al., 2010). The thinnest aluminum foil that could support itself without tearing, 0.8 μm, was selected to maximize the number of bombarding energies between 258.0 MeV and barrier. The Stopping and Range of Ions in Matter (SRIM) program was used to calculate the straggling and energy loss through the foils (Ziegler et al., 2010). The micron-level lateral straggling (less than 1.5 μm for all energies) was ignored considering the target size, and the kinetic energy loss was approximately linear in the energy domain. About 7 MeV was lost per degrader foil, giving four useful bombarding energies with up to three foils (including no degrader): 258.0 ± 0.5, 250.7 ± 1.8, 243.4 ± 3.7, and 236.0 ± 5.5 MeV. Due to a limited beam time of 2.5 days, 8 irradiations were done with duplicates of the 258.0 and 250.7 MeV bombarding energies. In addition, two commercial aluminum foils were used as targets to determine background from degrader foils.

Fig. 2 shows the blank flange with three 0.8 μm aluminum degrader foils stacked with four target mounting plates, including one for the yttrium, as indicated by the plate number in the photo. While the foils were commercially available, the mounting plates were custom made at the University of Notre Dame. A needle valve was attached to the Swagelok® fitting (seen to the right on the flange) to ensure pumping was slow enough not to damage the foils. Channels cut into the mounting plates and vented screws were also used to minimize trapped air in the system and ensure the thin foils would not rupture when the chamber was evacuated. The yttrium targets were purchased from ESPI Metals (Ashland, Oregon) with 99.9% purity and 25.4 mm × 25.4 mm × 1.016 mm in size. The aluminum degrader foils 30 mm × 30 mm × 0.0008 mm, with 99.1% purity were purchased from Goodfellow Metals (Coraopolis, Pennsylvania).

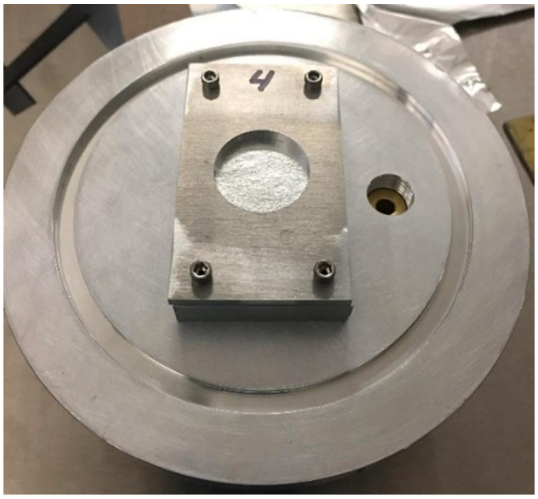

Fig. 2. Yttrium target mount with degrader foils.

Prior to irradiations, the beam was tuned on a phosphor plate placed within the mounting plates to ensure that the beam had the correct shape and alignment. After tuning was finished, a single yttrium target was placed in the foil stack holder, and the target station was sealed. During irradiation, unsuppressed Faraday cup measurements of beam current were taken and recorded at discrete points and used as averages for the duration of the run. Upstream current readings were taken in half-hour intervals during each irradiation and were scaled to a reading on a suppressed Faraday cup measured at the target position in the middle of the experiment. The periodic checks of the beam current allowed the beam to be generally monitored, but significant dips or spikes were not recorded. In future experiments, this will be addressed with a current integrator for beam delivery.

Table 1 shows the irradiation parameters for each of the targets as well as the averaged beam currents for each run. In addition to the yttrium reactions, two dedicated irradiations of aluminum foils were also performed to determine if any isotopes produced were from irradiation of either the degrader foils or the sides of the aluminum stack holder. The suppressed charge measurements varied between 7 and 12 electrical-nA, at a 15+ charge state. Beam intensity remains one of the largest systematic uncertainties in the analysis due to the lack of active charge integration during bombardment.

Following irradiation, offline counting of foils took place for several days. Target foils were placed at a fixed 15 cm source-to-detector distance which allowed for sufficient counting statistics and minimal deadtime (below 7%). The targets were counted several times in succession after end of beam (EoB) for 10-min acquisitions to capture short-lived residuals. A cooling period of 15 min was given before transporting the targets to the counting station. The gamma spectroscopy used Multichannel Analyzer Emulation Software (MAESTRO) in conjunction with an Al-windowed Ortec high-purity germanium (HPGe) detector (model GMX-70230-S) with a 20% relative efficiency and a full width at half maximum (FWHM) of 2.1 keV at 1408 keV. An Isotope Products Laboratories-certified 1.032 μCi ^{152}Eu source was used for energy and efficiency calibration at the same fixed 15 cm distance as the targets. Aluminum degrader foils were also screened. No activation products were observed by a Geiger counter or spectral analysis on the aluminum degrader foils, although residuals from aluminum reactions were observed in the yttrium targets.

3. Analysis

HPGe spectra were analyzed using FitzPeaks Gamma Analysis Software (JF Computing Services, 1981). The software package stored the efficiency and energy calibrations described and identified products via their characteristic gamma rays with a user-input library (Pritychenko et al., 2014). The software performed a self-consistency check on all gamma rays for a given nuclide and reported back a decay-corrected and background-subtracted activity for each 10-min spectrum. Table 2 lists the radionuclides and gamma lines of interest for this work (Pritychenko et al., 2014). Three reaction types were expected on both the yttrium target and aluminum degrader foils including fusion-fission and deep-inelastic transfer reactions on yttrium and fusion-evaporation on both yttrium and aluminum. Table 2 includes the observed isotopes and their reaction type.

Post processing of the spectra included confirming the library-assigned identity of radionuclides by allowing the half-lives to float as a fit parameter in the decay curves generated by successive HPGe spectra of the same target foil and comparing the fit values to published nuclear data (Pritychenko et al., 2014). Once radionuclide identification was confirmed, the published values were used in the EoB activity

Table 1
Irradiation specifications.

Run	Y 1	Y 2	Y 3	Y 4	Y 5	Y 6	Al 1	Al 2
Aluminum Foil Degraders	0	1	2	0	1	3	0	1
Energy Incident on Target Foil (MeV)	258.0 ± 0.5	250.7 ± 1.8	243.4 ± 3.6	258.0 ± 0.5	250.7 ± 1.8	236.0 ± 5.5	258.0 ± 0.5	250.7 ± 1.8
Irradiation Time (s)	14,400	23,520	28,860	21,600	23,460	43,080	3540	12,420
Averaged Irradiation Current (particle-nA)	0.92 ± 0.03	0.63 ± 0.04	0.78 ± 0.02	0.77 ± 0.03	0.68 ± 0.01	0.82 ± 0.01	0.82 ± 0.04	0.60 ± 0.05

Table 2
Observed isotopes.

Nuclide	Half Life	Target	Reaction Type	Gamma Ray Energy [keV] (Intensity)
^{148}Tb	1.0 h	^{89}Y	Fusion-evaporation	784 (84), 1079 (11)
^{149}Tb	4.12 h	^{89}Y	Fusion-evaporation	165 (26), 652 (16), 853 (16)
^{150}Tb	3.48 h	^{89}Y	Fusion-evaporation	638 (72), 67 (70)
^{73}Se	7.15 h	^{89}Y	Fusion-fission	361 (97)
^{74}Br	25.4 m	^{89}Y	Fusion-fission	635 (64), 219 (18), 634 (14)
^{74m}Br	46 m	^{89}Y	Fusion-fission	635 (91), 728 (36), 634 (16)
^{75}Br	96.7 m	^{89}Y	Fusion-fission	287 (88)
^{76}As	26.24 h	^{89}Y	Fusion-fission	559 (45), 657 (6)
^{76}Br	16.2 h	^{89}Y	Fusion-fission	559 (74), 657 (16)
^{76}Kr	14.8 h	^{89}Y	Fusion-fission	316 (39), 270 (21), 407 (12), 452 (10)
^{77}Br	57.04 h	^{89}Y	Fusion-fission	239 (23), 521 (22)
^{77}Kr	74.4 m	^{89}Y	Fusion-fission	130 (81), 147 (37)
^{90m}Y	3.19 h	^{89}Y	Deep-Inelastic Transfer	203 (97), 480 (91)
^{81}Rb	4.57 h	^{27}Al	Fusion-evaporation	190 (65), 446 (23)
^{83}Sr	32.41 h	^{27}Al	Fusion-evaporation	763 (27), 382 (14)
^{84}Y	39.5 m	^{27}Al	Fusion-evaporation	793 (98), 974 (78), 1040 (56), 661 (12)
^{85}Y	2.68 h	^{27}Al	Fusion-evaporation	232 (84), 504 (60)
^{85m}Y	4.86 h	^{27}Al	Fusion-evaporation	232 (23)
^{86}Y	14.74 h	^{27}Al	Fusion-evaporation	1077 (83), 628 (33), 1153 (31), 777 (22)
^{86m}Y	47.4 m	^{27}Al	Fusion-evaporation	208 (94)
^{87}Y	79.8 h	^{27}Al	Fusion-evaporation	484 (90), 388 (82)
^{87m}Y	13.37 h	^{27}Al	Fusion-evaporation	381 (78)
^{86}Zr	16.5 h	^{27}Al	Fusion-evaporation	243 (96)

calculations.

Table 2 shows the user input library for a library driven analysis of observed gamma-ray energies (Pritychenko et al., 2014). For radionuclides with several decay signatures, the list was capped at four energies with intensity greater than 5%. Despite the prominence of the 352 keV gamma ray from ^{149} Tb day with 29% intensity, it was not used to determine yields due to an overlapping and inconsistent background line of ^{214}Pb and thus not included in the table above. ^{76}As and ^{76}Br were resolved through an analysis of a ratio of observed gamma rays as well as experimental half-lives accounting for ingrowth of ^{76}Br from ^{76}Kr. Low terbium activities and the long-lived nature of daughter products prevented the observation of any gadolinium activities.

4. Results

The PACE4 simulated cross-sections for the mass distributions following nucleon evaporation from the compound nucleus ^{152}Er are displayed in Fig. 3. For the A = 146 mass chain, the terbium isotope has an 8-s half life. This curve therefore represents the daughter, ^{146}Gd,

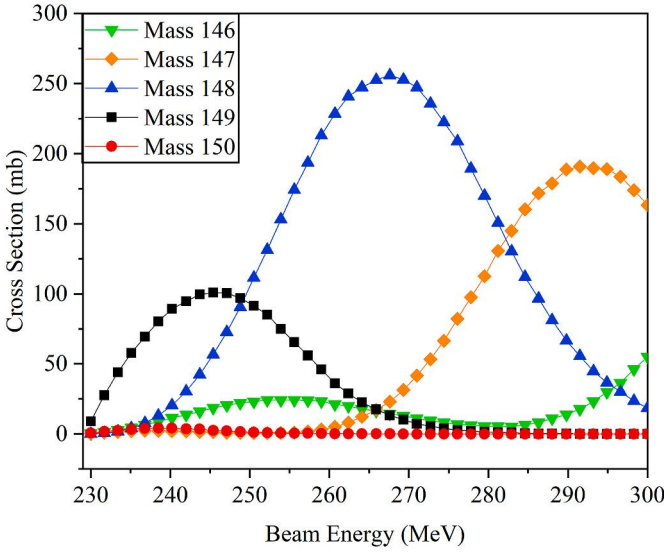

Fig. 3. Simulated cross section (from LISE++) plot for 5 isobars.

which is coproduced in small abundances but is chemically separable. For all other mass chains, the curves represent the direct and indirect production of terbium isotopes. For the mass-149 isobar, production is mostly via the (*p*,2*n*) exit channel leading to ^{149}Ho. Secondary contributions are via ^{149}Er, while ^{149}Dy is simulated to be a constant 9% across the experimental energy range. Direct production of both isomers of ^{149}Tb was negligible. Deep-inelastic (DI) transfer reactions were not studied with this model but likely occur (Rivet et al., 1979).

Using the simulated cross section data, a modeled physical yield was derived for the energetically thick target for all predicted reactions at the bombarding energy down to barrier. The EoB thick-target yields (TTY) in Bq/μAh were calculated according to the following equation:

$$TTY = \frac{\phi \rho N_A}{A}\left(1 - e^{-\lambda t}\right) \int_{C.B.}^{E_{in}} \frac{\sigma(E)}{\frac{dE}{dx}} dE$$

where ϕ is the incident particle flux, ρ and A are the density and molar mass respectively of the target, N_A is Avogadro's constant, t is the irradiation time, $\sigma(E)$ is the cross section parameterized in energy across the integration limits of bombarding energy (E_{in}) down to the Coulomb barrier ($C.B.$) and $\frac{dE}{dx}$ is stopping power as a function of energy. There is no correction for target purity because yttrium is naturally monoisotopic. SRIM was used to model the stopping power and projected range where the beam remains above the Coulomb barrier for the desired reactions. The SRIM uncertainties were not included in the forward calculations but can contribute up to 22% more uncertainty to each of the simulated curves (Ziegler et al., 2010). The bombarding energy uncertainty is mostly attributed to commercial thickness uncertainties in the aluminum degrader foils. Fig. 4 plots these simulated yields as solid curves with the experimental data overlaid. The relative strength of the A = 149 isobar's simulated production is clear below bombarding energies of 240 MeV, although experimental values do not support this. The tabular values of experimental yields are shown in

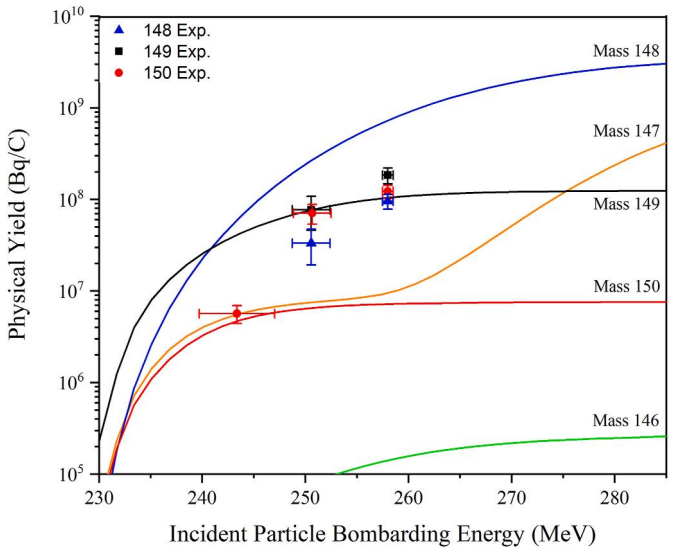

Fig. 4. Experimental & theoretical thick-target physical yields.

Table 3.

Table 3 lists singular values at 258.0 and 250.7 MeV because the yields at these duplicate irradiation energies were averaged. There were no observed fusion-evaporation residues at 236.0 MeV, the lowest bombarding energy. Only ^{150}Tb was observed at 243.4 MeV as the other terbium isotopes were below the limit of detection (LOD). ^{149}Tb had a LOD of 370 Bq; ^{148}Tb had a LOD of 70 Bq, and ^{150}Tb had a LOD of 240 Bq. The differences in LOD are attributed to the underlying branching ratios of the nuclides and the background across the channels of the observed gamma rays (Knoll, 2010). The energetically thick targets in this experiment match well with conditions that would be used to produce radionuclides for medical applications. While cross section measurements at discrete excitation energies are not possible without thin targets, the high measured yields are encouraging motivation for future work with energetically thin targets.

Fig. 4 is consistent with the statistical evaporation trends at increased energies but the simulations differ significantly from the experimental results. ^{149}Tb marginally had the highest physical yields when produced at 250.7 and 258.0 MeV, and ^{150}Tb was severely underpredicted by the PACE4 code. The experimental results show the resolution of the exit channels is not as sharp as PACE4 predicts. For a thick target, the production of ^{150}Tb is inevitable, but future thin target work could minimize this if the target is thin enough to limit near barrier reactions. The A = 150 mass chain does show some leveling off from a peak, but both the 148 and 149 mass chains will require more data to determine their trends.

The observed physical yields of side products are shown in Table 4. The associated uncertainty is given in parentheses. In addition to fusion-evaporation reactions, the additional excitation energies of the compound nucleus ranged from 45 to 60 MeV for the various bombarding energies studied here. This excitation appears to have opened the fission reaction pathway that becomes more symmetric closer to the coulomb barrier. A GEMINI++ calculation supports this open channel at the simulated excitation energies. GEMINI++ is a Monte-Carlo code for modeling the binary decay of compound nuclei, with particular focus on complex-fragment emission in heavy-ion fusion systems with symmetric fission also considered (Charity, 2008). Due to the high lab energies and momenta, a dynamical reaction such as a fusion-fission channel is proposed as the reason the six most common radionuclides listed in Table 4 were observed in this reaction. Perfectly symmetric fission of the ^{152}Er compound nucleus results in two ^{76}Se nuclei. The observed distribution products apart from the intended Tb isotopes were all near this symmetric mass number, but not all distribution products were observable by gamma-ray spectroscopy. Several stable or long-lived nuclei are the counterparts to many observed products in either complete fission or a fission-*xn* exit channel. At the highest bombarding energy, 258.0 MeV, another nuclide, ^{90m}Y was observed. This high-spin isomer was produced via a one nucleon transfer to the target material, ^{89}Y. It is best understood as a deep-inelastic transfer reaction.

5. Discussion

Our studies show that the heavy ion route is feasible for production of the medically useful ground state of ^{149}Tb, but raw yields reported here do not compete with light-ion spallation reactions and there is still the presence of terbium contaminants ^{148}Tb and ^{150}Tb. The PACE4 predictions of high cross sections appears to be mitigated by the high stopping powers of a near-symmetric reaction. Despite limiting formation of longer-lived terbium contaminants, this reaction route's measured physical yields are smaller than established spallation methods (see Table 5). This reaction also supports fusion-fission considerations in other heavy-ion and near-symmetric approaches. Test productions for research would require development of radiochemical isolation techniques.

Using SRIM modeling to estimate the target thickness, the ^{63}Cu ion movement through the target while still greater than the Coulomb barrier, is in the micrometer range. At the maximum bombarding energy tested, 258.0 MeV, the projected range of ^{63}Cu ions before falling below the energy to overcome the Coulomb barrier of the ^{89}Y nucleus is 3.1 μm. From a purity standpoint, a thinner foil could be easily implemented and would decrease the production of much of the ^{150}Tb produced close to barrier. Using the experimental observations, thinner targets allowing the beam to exit the yttrium target with an energy of 243.4 MeV would not detract from ^{149}Tb production but would minimize the ^{150}Tb contributions. The stopping range for heavy ions is also much shorter than for GeV-proton spallation reactions, 3 μm vs. several millimeters, which could justify the difference between lower production activities for the heavy-ion approach. The target recovery yield could potentially be much higher with less material to process and fewer residuals to

Table 4
Tabular fusion-fission products physical yields (MBq/μAh).

Energy	258.0 MeV	250.7 MeV	243.4 MeV	236.0 MeV
Se-73	0.97 (0.08)	0.70 (0.07)	0.48 (0.06)	–
Br-74m	0.31 (0.03)	0.32 (0.04)	0.24 (0.17)	–
Br-75	0.38 (0.03)	0.25 (0.03)	0.13 (0.2)	–
Kr-76	1.03 (0.34)	1.40 (0.32)	0.73 (0.59)	0.42 (0.05)
Kr-77	1.00 (0.11)	1.04 (0.14)	0.89 (0.21)	–
As-76	5.20 (0.44)	3.72 (0.46)	3.07 (0.40)	1.85 (0.23)
Y-90m	0.05 (0.01)	–	–	–

Table 3
EoB thick-target physical yields.

Energy (MeV)	Physical Yield ^{148}Tb (MBq/μAh)	EoB ^{148}Tb Activity (Bq)	Physical Yield ^{149}Tb (MBq/μAh)	EoB ^{149}Tb Activity (Bq)	Physical Yield ^{150}Tb (MBq/μAh)	EoB ^{150}Tb Activity (Bq)
258.0 ± 0.5	0.34 (.06)	1347 (133)	0.66 (0.13)	1537 (150)	0.44 (0.07)	1126 (61)
250.7 ± 1.8	0.12 (0.05)	535 (203)	0.28 (0.11)	842 (314)	0.25 (0.06)	843 (123)
243.4 ± 3.6	<LOD	<LOD	<LOD	<LOD	0.02 (0.004)	102 (19)
236.0 ± 5.5	<LOD	<LOD	<LOD	<LOD	<LOD	<LOD

Table 5
Main production routes of ^{149}Tb (Moiseeva et al., 2020).

Reaction Channel	Projectile Energy (MeV)	Compound Nucleus	Yield (MBq/μAh)	Reference
^{152}Gd (p,4n)^{149}Tb	70–30	^{153}Tb	2600	Steyn et al., 2014
^{151}Eu (^{3}He,5n)^{149}Tb	70–40	^{154}Tb	19.4	Zagryadskii et al., 2017
^{151}Eu (^{3}He,5n)^{149}Tb	70–30	^{154}Tb	38.7	Moiseeva et al., 2020
^{142}Nd (^{12}C,5n)^{149}Dy →^{149}Tb	108	^{154}Dy	3.3	Zaitseva et al., 2003
^{141}Pr (^{12}C,4n)^{149}Tb	71.5	^{153}Tb	0.086	Maiti, 2011
^{nat}Ta (p,x)^{149}Tb	1000–1400	^{182}W	~3000	Beyer et al., 2002
^{89}Y (^{63}Cu,$xnyp$)^{149}X→^{149}Tb	258.0	^{152}Er	0.66	This work

separate. Decreasing the thickness of the target reduces the mass manipulation in any future chemical separations and thin yttrium targets might tolerate increased beam intensities.

The copper-ion production and subsequent transmission of this heavy-ion beam could be increased as a first step to increase overall EoB yields. A dedicated cyclotron for heavy-ion beams in the 3–7 MeV/A range could also access this and other reactions for the production of proton-rich radionuclides. Despite these potential upgrades, copper-ion beam availability and beam intensity are the largest hurdles for this heavy-ion approach. Medically useful radionuclides are attainable with heavy-ion production channels not possible with light-ion cyclotrons and demanding higher beam intensities than most tandem accelerators can provide (McGuinness et al., 2021). An ion source designed for copper beams would significantly increase production currents.

As separation chemistry would enable isolation of elemental terbium, this preliminary work was focused on the production of terbium isotopes as opposed to isotopes of other elements (Kazakov et al., 2018; Brezovcsik et al., 2018). Previous work, on which the modeling software is based, shows that the barrier may have a large degree of uncertainty when applied to dynamical events like deep-inelastic transfer reactions and fission events (Gavron, 1980). Observed gamma rays from nuclei with few nucleon transfers between the target and beam, such as ^{90m}Y, support the DI channel that were not initially anticipated. The fusion-evaporation software is not encompassing of dynamical reactions.

Credit author statement

John T. Wilkinson: Conceptualization, Methodology, Validation, Formal analysis, Investigation, Writing – Original Draft, Writing – Review & Editing, Visualization. Kendall E. Barrett: Formal analysis, Investigation, Writing – Original Draft, Writing – Review & Editing; Samuel J. Ferran: Formal analysis, Investigation, Writing – Original Draft, Writing – Review & Editing; Sean R. McGuinness: Conceptualization, Methodology, Software, Formal analysis, Investigation, Data Curation, Writing – Review & Editing; Mallory McCarthy: Investigation, Writing – Review & Editing; Lauren McIntosh: Investigation, Resources, Writing – Review & Editing; Sherry J. Yennello: Investigation, Resources, Writing – Review & Editing, Funding acquisition; Jonathan W. Engle: Writing – Review & Editing, Supervision, Project administration; Suzanne E. Lapi: Conceptualization, Methodology, Investigation, Resources, Writing – Review & Editing, Supervision, Project administration; Graham F. Peaslee: Conceptualization, Methodology, Investigation, Resources, Writing – Review & Editing, Supervision, Project administration, Funding acquisition.

Declaration of competing interest

The authors declare that they have no known competing financial interests or personal relationships that could have appeared to influence the work reported in this paper.

Acknowledgements

We would like to thank all involved parties in making this work possible. Specifically, Jerry Lingle at the University of Notre Dame for his help in target holder machining, the Texas A&M Cyclotron Institute staff for delivering beam to target, and Bob Charity for his helpful discussions of the quasi-fission channels and for performing the GEMINI++ calculation.

We would also like to thank our funding source for helping make this possible. This work was supported by the U.S. Department of Energy, Office of Science, Office of Nuclear Physics, DOE Isotope Program, United States, under a funded proposal from DE-SC0013452, The DOE, Office of Science – Nuclear Physics under award DEFG02-93ER40773, Department of Energy, National Nuclear Security Administration, under Award Number DE-NA0003841.

References

Aghevlian, S., Boyle, A.J., Reilly, R.M., 2017. Radioimmunotherapy of cancer with high linear energy transfer (LET) radiation delivered by radionuclides emitting α-particles or Auger electrons. Adv. Drug Deliv. Rev. 109, 102–118.

Allen, B.J., Blagojevic, N., 1996. Alpha-and beta-emitting radiolanthanides in targeted cancer therapy: the potential role of terbium-149. Nucl. Med. Commun. 17 (1), 40–47.

Beyer, G.J., Čomor, J.J., Daković, M., Soloviev, D., Tamburella, C., Hagebø, E., Allan, B., Dmitriev, S.N., Zaitseva, N.G., 2002. Production routes of the alpha emitting 149Tb for medical application. Radiochim. Acta 90 (5), 247–252.

Beyer, G.J., Miederer, M., Vranješ-Đurić, S., Čomor, J.J., Kuenzi, G., Hartley, O., Senekowitsch-Schmidtke, R., Soloviev, D., Buchegger, F., 2004. Targeted alpha therapy in vivo: direct evidence for single cancer cell kill using 149Tb-rituximab. Eur. J. Nucl. Med. Mol. Imag. 31 (4), 547–554.

Brezovcsik, K., Kovács, Z., Szelecsényi, F., 2018. Separation of radioactive terbium from massive Gd targets for medical use. J. Radioanal. Nucl. Chem. 316 (2), 775–780.

Browne, E., Tuli, J.K., 2009. Nuclear data sheets for A= 145. Nucl. Data Sheets 110 (3), 507–680.

Charity, R., 2008. GEMINI: a Code to Simulate the Decay of a Compound Nucleus by a Series of Binary Decays (No. INDC (NDS)–0530).

Duchemin, C., Guertin, A., Haddad, F., Michel, N., Métivier, V., 2016. Deuteron induced Tb-155 production, a theranostic isotope for SPECT imaging and auger therapy. Appl. Radiat. Isot. 118, 281–289.

Duchemin, C., Ramos, J.P., Stora, T., Aubert, E., Audouin, N., Barbero, E., Barozier, V., Bernardes, A.P., Bertreix, P., Boscher, A., Burnel, D., 2020. May. Cern-medicis: a unique facility for the production of nonconventional radionuclides for the medical research. In: 11th International Particle Accelerator Conference.

Firestone, R.B., Shirley, V.S., Baglin, C.M., Chu, S.Y.F., Zipkin, J., 1996. Table of Isotopes, eighth ed., vol. II

Gavron, A., 1980. Statistical model calculations in heavy ion reactions. Phys. Rev. C 21 (1), 230.

JF Computing Services. FitzPeaks gamma analysis and calibration software version 3.62, UK, October 2016. Based on methods described in: Koskelo, M.J., Aarnio, P.A. and Routti, J.T., 1981. SAMPO80: an Accurate Gamma Spectrum Analysis Method for Minicomputers. Nuclear Instruments and Methods in Physics Research, vol. 190(1), pp.89-99.

Kazakov, A.G., Aliev, R.A., Bodrov, A.Y., Priselkova, A.B., Kalmykov, S.N., 2018. Separation of radioisotopes of terbium from a europium target irradiated by 27 MeV α-particles. Radiochim. Acta 106 (2), 135–140.

Knoll, G.F., 2010. Radiation Measurement and Detection. John Wiley & Sons, 1.

Macfarlane, R.D., 1962. Alpha-Emitting Isomeric State of Tb149. Phys. Rev. 126 (1), 274–276.

Maiti, M., 2011. New measurement of cross sections of evaporation residues from the natPr+ 12C reaction: a comparative study on the production of 149Tb. Phys. Rev. C 84 (4), 044615.

McDevitt, M.R., Sgouros, G., Finn, R.D., Humm, J.L., Jurcic, J.G., Larson, S.M., Scheinberg, D.A., 1998. Radioimmunotherapy with alpha-emitting nuclides. Eur. J. Nucl. Med. 25 (9), 1341–1351.

McGuinness, S.R., Ferran, S.J., Wilkinson, J.T., Loveless, C.S., Anderson, T., Blankstein, D., Clark, A.M., Henderson, S.L., Nelson, A.D., Reingold, C.S., Skulski, M., 2021. Production of 52Fe from symmetric complete fusion-evaporation reactions. Nucl. Instrum. Methods Phys. Res. Sect. B Beam Interact. Mater. Atoms 493, 15–18.

Moiseeva, A.N., Aliev, R.A., Unezhev, V.N., Zagryadskiy, V.A., Latushkin, S.T., Aksenov, N.V., Gustova, N.S., Voronuk, M.G., Starodub, G.Y., Ogloblin, A.A., 2020. Cross section measurements of 151Eu (3He, 5n) reaction: new opportunities for medical alpha emitter 149Tb production. Sci. Rep. 10 (1), 1–7.

Morton III, J.R., Choppin, G.R., Harvey, B.G., 1962. Study of the reactions $Pr^{141}(C^{12}, 4n)Tb^{149}$ and $Te^{130}(C^{12}, 5n)Ce^{137m}$ by means of recoil techniques. Phys. Rev. 128 (1), 265.

Müller, C., Fischer, E., Behe, M., Köster, U., Dorrer, H., Reber, J., Haller, S., Cohrs, S., Blanc, A., Grünberg, J., Bunka, M., 2014. Future prospects for SPECT imaging using the radiolanthanide terbium-155—production and preclinical evaluation in tumor-bearing mice. Nucl. Med. Biol. 41, e58–e65.

Müller, C., Vermeulen, C., Köster, U., Johnston, K., Türler, A., Schibli, R., van der Meulen, N.P., 2017. Alpha-PET with terbium-149: evidence and perspectives for radiotheragnostics. EJNMMI radiopharmacy and chemistry 1 (1), 1–5.

Naskar, N., Lahiri, S., 2021. Theranostic terbium radioisotopes: challenges in production for clinical application. Front. Med. 8.

Poty, S., Francesconi, L.C., McDevitt, M.R., Morris, M.J., Lewis, J.S., 2018a. α-Emitters for radiotherapy: from basic radiochemistry to clinical studies—Part 1. J. Nucl. Med. 59 (6), 878–884.

Poty, S., Francesconi, L.C., McDevitt, M.R., Morris, M.J., Lewis, J.S., 2018b. α-Emitters for radiotherapy: from basic radiochemistry to clinical studies—part 2. J. Nucl. Med. 59 (7), 1020–1027.

Pritychenko, B., Běták, E., Singh, B., Totans, J., 2014. Nuclear science references database. Nucl. Data Sheets 120, 291–293.

Radiation Effects Facility, 2020. Texas A&M University, Cylotron Institute. https://cyclotron.tamu.edu/ref/images/brochure_2020.pdf (accessed 27 April 2021).

Rivet, M.F., Bimbot, R., Gardès, D., Fleury, A., Hubert, F., Llabador, Y., 1979. Production of 149gTb in deep inelastic transfer reactions: an approach to the angular momentum of fragments. Zeitschrift für Physik A Atoms and Nuclei 290 (1), 57–66.

Steyn, G.F., Vermeulen, C., Szelecsényi, F., Kovács, Z., Hohn, A., van der Meulen, N.P., Schibli, R., Van der Walt, T.N., 2014. Cross sections of proton-induced reactions on 152Gd, 155Gd and 159Tb with emphasis on the production of selected Tb radionuclides. Nucl. Instrum. Methods Phys. Res. Sect. B Beam Interact. Mater. Atoms 319, 128–140.

Tabacaru, G., Clark, H., Arje, J., May, D., 2019. Cyclotron Institute at Texas A&M university: a facility overview, 1. In: AIP Conference Proceedings, vol. 2076. AIP Publishing LLC, 040002.

Tarasov, O.B., Bazin, D., 2003. Development of the program LISE: application to fusion–evaporation. Nucl. Instrum. Methods Phys. Res. Sect. B Beam Interact. Mater. Atoms 204, 174–178.

Zagryadskii, V.A., Latushkin, S.T., Malamut, T.Y., Novikov, V.I., Ogloblin, A.A., Unezhev, V.N., Chuvilin, D.Y., 2017. Measurement of terbium isotopes yield in irradiation of 151Eu targets by 3He nuclei. Atom. Energy 123 (1), 55–58.

Zaitseva, N.G., Dmitriev, S.N., Maslov, O.D., Molokanova, L.G., Starodub, G.Y., Shishkin, S.V., Shishkina, T.V., Beyer, G.J., 2003. Terbium-149 for nuclear medicine. The production of 149Tb via heavy ions induced nuclear reactions. Czech. J. Phys. 53 (1), A455–A458.

Ziegler, J.F., Ziegler, M.D., Biersack, J.P., 2010. SRIM–The stopping and range of ions in matter (2010). Nucl. Instrum. Methods Phys. Res. Sect. B Beam Interact. Mater. Atoms 268 (11–12), 1818–1823.